Int. J. Electrochem. Sci., 12 **(2017)** 7557 – 7569, doi: 10.20964/2017.08.49

International Journal of ELECTROCHEMICAL SCIENCE
www.electrochemsci.org

Graphene-Gold Nanoparticles Nanohybrids for Electrochemical Detection of Malachite Green

Xiu-Chun Guo[1,†,*], *Xuan Cao*[2,†], *Hai-Hui Wang*[3], *Meng Yuan*[3], *Xuan-Jie Chen*[1], *Wen-Yi Kang*[1], *Wen-Hui Zhou*[3,**]

[1] Institute of Chinese Materia Medica, Henan University, Kaifeng 475004, China.
[2] Institute of Oceanographic Instrumentation, Shandong Academy of Sciences, Qingdao 266061, China.
[3] the Key Laboratory for Special Functional Materials of MOE, Henan University, Kaifeng 475004, China.
[*]E-mail: guoxiuchun@henu.edu.cn
[**]E-mail: zhouwh@henu.edu.cn, zhouwh@foxmail.com
† These two authors contributed equally to this work.

Received: 27 April 2017 / *Accepted:* 8 June 2017 / *Published:* 12 July 2017

Malachite green (MG) was an important bactericide and is now banned in different countries due to it's bad effect to human health. In this work, graphene-gold nanohybrids (Graphene-GNPs) were prepared by the chemical co-reduction of Au (III) and graphene oxide (GO) with sodium citrate. These Graphene-GNPs were characterized by TEM, SEM, XRD and EDS. After deposition on glassy carbon electrode (GCE), an electrochemical sensor was proposed for the electrochemical detection of MG. The electrocatalytic oxidation of MG on Graphene-GNPs modified GCE (Graphene-GNPs/GCE) was investigated by differential pulse voltammetry (DPV), cyclic voltammetry (CV) and electrochemical impedance spectroscopy (EIS). The results showed that the Graphene-GNPs could enhance the electrochemical detection performance towards oxidation of MG. Under the optimized condition, the constructed MG electrochemical sensor showed linear dynamic range from 0.1 μm to 800 μM. Moreover, the proposed MG electrochemical sensor has also been successfully used for MG determination in real water samples with satisfied recoveries (97.5 % to 109.6 %) and precision (0.35 % to 5.57 %).

Keywords: Malachite green; MG; Graphene-Gold nanoparticles nanohybrids; Electrochemical detection; electrochemical sensor.

1. INTRODUCTION

Malachite green (MG) is a kind of well-known cationic triphenylmethane dye [1], which is widely used in silk, leather and paper dyeing, as well as cell staining [2-4]. As effective and cheap anti-

fungal and anti-microbial agent, MG also has been extensively used in aquaculture industry over the world [5-7]. Since 1990s, lots of studies have suggested that MG is highly toxic to microbial and mammalian cells, promoting the hepatic tumor formation in rodents and reproductive abnormalities in rabbits and fish [8-9]. In addition, MG is believed to have potential mutagenicity, teratogenicity, genotoxicity and carcinogenicity to humans. So, the use of MG is banned all over the world, including China, USA and European Union [10]. However, MG was often illegally used in aquaculture industry due to the low cost, easy availability, high efficacy against fungus, bacteria and parasite [11]. Therefore, a simple, reliable, rapid, sensitive and selective method for the determination of MG in aquatic products is highly demanded. Up to now, several kinds of methods have been developed for the detection of MG including electrochemical method [12], high performance liquid chromatography (HPLC) [13], liquid chromatography-mass spectrometry (LC-MS) [14], surface-enhanced Raman spectroscopy (SERS) [15], spectrophotometric method [16] and Enzyme-linked immunoassay [17]. Among these methods, electrochemical method gained much more interest due to the advantages of great speed, simplicity, low cost and short analysis time [18-20].

As a two-dimensional sheet composed of sp^2-bonded carbon atoms, graphene has recently attracted tremendous attention due to its unique thermal, mechanical and electrical properties [21-23]. For example, graphene can be used as electrode modified material for construction of high-performance electrochemical sensors or biosensors [24-25]. Many important studies also had shown that the combination of graphene with other metal nanoparticles (NPs) offer opportunities for developing graphene-based hybrids as enhanced materials to construct newly high-performance electrochemical sensing platforms [26]. On the other hand, noble metal NPs also had been widely used for the preparation of nanocomposites for electrochemical sensor [27]. Noble metal NPs often have many excellent properties, such as large surface-to-volume ratio, good electrical properties, strong adsorption ability, high surface reaction activity, small particle size and good surface properties [28]. Among the diverse noble metal NPs, gold nanoparticles (GNPs) have received extensive study due to their unique properties, including high electrical conductivity and excellent electrocatalytic activity [29]. Recently, graphene-gold nanoparticles (Graphene-GNPs) nanohybrids have been attempted to modify the electrode to design highly sensitive, selective and stable electrochemical sensors [30].

In this work, a simple, fast, convenient and sensitive electrochemical sensor was developed for the determination of MG using Graphene-GNPs nanohybrids. The Graphene-GNPs nanohybrids were obtained by the simultaneous and in-situ chemical co-reduction of Au (III) and GO using sodium citrate. Subsequently, a sensitive electrochemical sensor for MG detection was fabricated by deposition of Graphene-GNPs nanohybrids on glass carbon electrode (Scheme 1). The Graphene-GNPs nanohybrids were characterized by using SEM, TEM, XRD and EDS. Due to the synergistic effect of graphene and GNPs, the Graphene-GNPs based electrochemical sensor significantly enhanced the DPV current response and selectivity towards MG. To the best of our knowledge, this work represents the first attempt using graphene and GNPs nanohybrids for the fabrication of electrochemical sensor for MG detection.

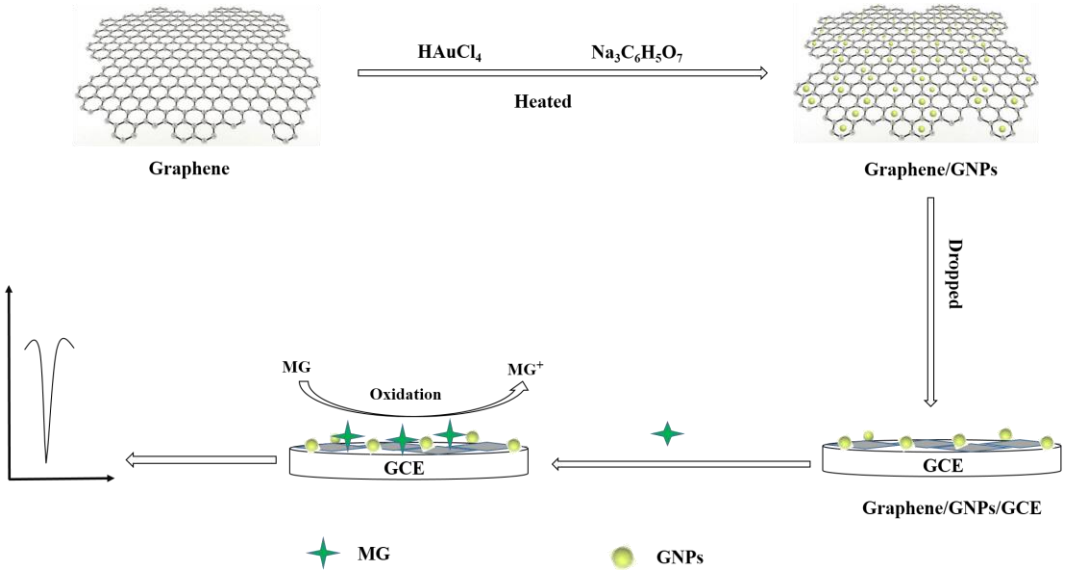

Scheme 1. Schematic illustration of the procedure for synthesis of Graphene-GNPs nanohybrids and use for electrochemical MG detection

2. EXPERIMENTAL

2.1. Apparatus and Materials

The transmission electron microscopy (TEM) images were obtained on a JEOL JEM-2010 transition electronic microscopy with an accelerating voltage of 200 kV. The scanning electron microscope (SEM) observation was performed on an FEI Nova NanoSEM 450 field emission scanning electron microscope (FESEM). The powder X-ray diffraction (XRD) patterns were carried out using a Bruker D8 Advance X-ray diffractometer. Energy dispersive X-ray spectroscopy (EDS) analysis was performed using accessory (INCA 250) of Nova NanoSEM 450 instrument. Electrochemical measurements such as differential pulse voltammetry (DPV), cyclic voltammetry (CV) and electrochemical impedance spectroscopy (EIS) were all performed on CHI660E electrochemical workstation (Chen Hua Instruments Co., Shanghai, China).

Mountain green (MG), chloroauric acid ($HAuCl_4$) and flake graphite were obtained from Alfa Aesar. Unless stated otherwise, all other chemicals were of analytical reagent grade and used as received. All the ultrapure water used in this work was obtained from a Milli-Q purification system (Millipore, Bedford, MA).

2.2. Synthesis of Graphene-GNPs Nanohybrids

Graphene oxide (GO) was synthesized from natural flake graphite using Hummers method [31]. The prepared graphite oxide was then exfoliated in ultrapure water by ultrasonication to form a 1.0 mg/mL homogeneous graphene oxide colloidal dispersion as before [26]. The Graphene-GNPs nanohybrids were prepared as follow: firstly, 1.25 mL of 1.0 mg/mL GO dispersion was mixed with 25

mL of 0.48 mM of $HAuCl_4$ aqueous solution in round-bottom flask. After continued ultrasonication for 30 min, 470 μL of 85 mM sodium citrate was added to the above solution. Then the round-bottom flask was placed in a water bath and stabled at 85 ^oC for 60 min, obtaining stable black Graphene-GNPs nanohybrids dispersion. The Graphene-GNPs nanohybrids were washed several times by centrifugation and ultrasonication. The preparation of GNPs and graphene was similar to that of Graphene-GNPs nanohybrids but without the addition of GO or $HAuCl_4$.

2.3. Fabrication of Graphene-GNPs Nanohybrids modified GCE electrode

Before surface modification, the glassy carbon electrode (GCE) was polished to a mirror-like surface with 0.3 μm and 0.05 μm alumina slurry. After subsequently ultrasonicated in ethanol and ultrapure water, the pretreated GCE was dried with high-purity argon gas. As shown in Scheme 1, surface modification was commenced by applying a 10 μL aliquot dispersion of the resulting Graphene-GNPs nanohybrids on GCE and dried under infrared lamp for 10 min. The fabrication of graphene and GNPs modified GCE electrode were similarly to that of Graphene-GNPs nanohybrids modified GCE electrode.

3. RESULTS AND DISCUSSION

3.1. Characterization of graphene and Graphene-GNPs nanohybrids

In this work, Graphene-GNPs nanohybrids were prepared by the chemical co-reduction of Au (III) and GO with sodium citrate [32]. The surface morphology of graphene as well as successful loading of GNPs on graphene were confirmed by TEM and SEM. Figure 1a shows the typical TEM image of graphene sheet with no aggregation. Figure 1b is the TEM image of prepared Graphene-GNPs nanohybrids, indicating Graphene-GNPs nanohybrids could be synthesized in one pot by chemical co-reduction using sodium citrate.

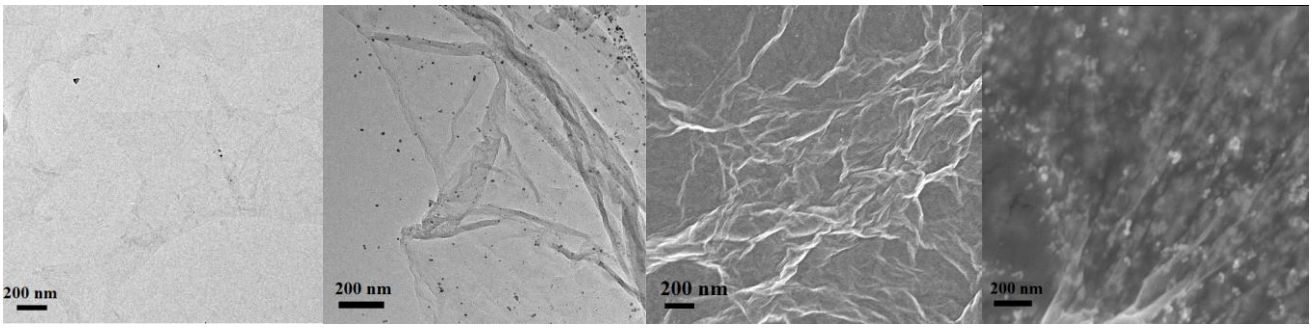

Figure 1. The TEM images of graphene and Graphene-GNPs nanohybrids (a, b); the SEM images of graphene and Graphene-GNPs nanohybrids (c, d).

It can be seen that GNPs with diameter 5~20 nm are successfully loaded on the whole surface of graphene, though the dispersion is heterogeneous. The reason might be attributed to the stirring inhomogeneity during formation of GNPs on graphene. The TEM images of graphene and Graphene-GNPs nanohybrids on GCE are shown in Figure 1c and 1d. Both of graphene and Graphene-GNPs nanohybrids show typical crumpled and wrinkled structure with multi-layer on the surface of GCE. The geometric wrinkling may arise from π-π interaction within sheets of graphene not only minimizes the surface energy but also induces mechanical integrity with tensile strength [33]. The presence of discrete GNPs on the surface of graphene remarkably suppressed the wrinkling of graphene.

XRD is also an effective technique used for study the interlayer modifications induced in graphene based hybrids. Figure 2a shows the XRD patterns of GNPs, graphene oxide and Graphene-GNPs nanohybrids, respectively. Clearly, we observe four well defined Au XRD feature peaks for (111) at about 38°, (200) at about 44°, (220) at about 65° and (311) at about 78°, which are consistent with the face centered cubic Au (JCPDS, No. 4-0784) [34]. Freshly exfoliated graphene oxide exhibits sharp diffraction peak located at about 11 °, corresponding to the (002) inter-planar spacing around 0.8 nm [35]. Generally, graphene obtained from chemical reduction of graphene oxide often exhibits broad peak at around 25 ° due to the aggregation of graphene (to form graphite spontaneously and slowly). As for Graphene-GNPs nanohybrids, the Bragg angles of 38 °, 44 °, 65 ° and 78 ° for GNPs were also clearly observed, which confirm the successful loading of GNPs on graphene. In addition, the GNPs suppress the aggregation of graphene. The EDS characterization of Graphene-GNPs nanohybrids was further performed to reveal the composition of Graphene-GNPs nanohybrids. As shows in Figure 2b, carbon, oxygen and gold are detected, suggesting the successful integration of graphene and GNPs in nanohybrids.

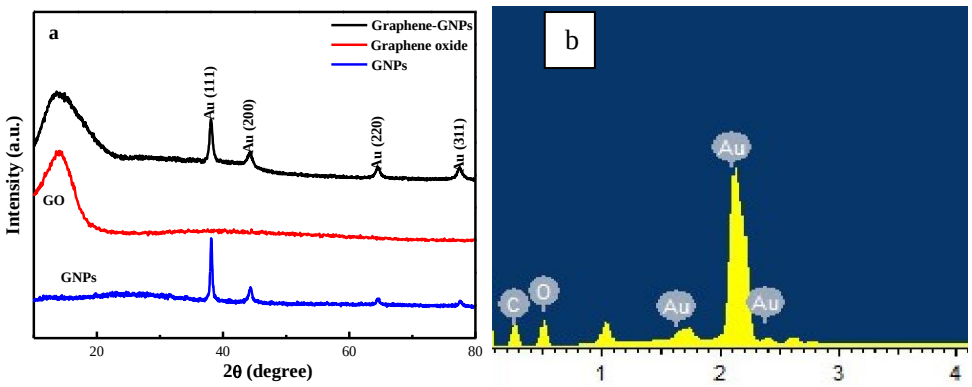

Figure 2. XRD patterns of GNPs, Graphene oxide and Graphene-GNPs nanohybrids (a); EDS elemental analysis of Graphene-GNPs nanohybrids (b).

3.2. Electrochemical behavior of MG on different materials modified GCE

The electrochemical response of different materials modified GCE toward MG was studied by DPV method. As shown in Figure 3, all the modified GCE displayed higher DPV current response than that of bare GCE. The peak currents of MG on bare GCE, graphene/GCE, GNPs/GCE and

Graphene-GNPs/GCE are 3.365, 4.236, 4.924 and 6.719 μA, respectively. The oxidation peaks of MG on bare GCE, GNPs/GCE, graphene/GCE and Graphene-GNPs/GCE were observed at 0.797 V, 0.791 V, 0.789V and 0.787 V, respectively. Obviously, the DPV peak on Graphene-GNPs/GCE show the lowest potential than that of bare GCE, GNPs/GCE and graphene/GCE. This result indicated that the Graphene-GNPs nanohybrids possess higher catalytic activity than graphene and GNPs, as well as bare GCE [26]. This also further indicated that the Graphene-GNPs nanohybrids could be used for the fabrication of electrochemical sensor for MG determination.

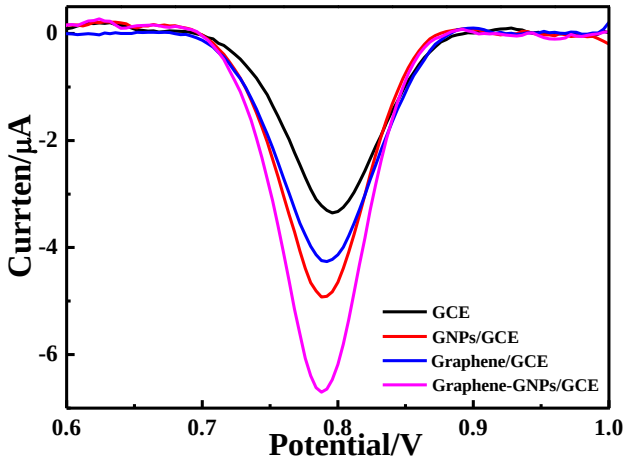

Figure 3. DPV responses of bare GCE, GNPs/GCE, graphene/GCE and Graphene-GNPs/GCE immersed in 200 μM MG solution.

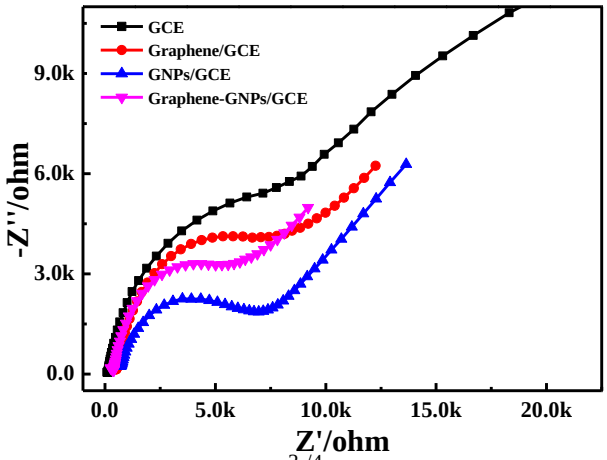

Figure 4. EIS recorded in 0.01 M $[Fe(CN)_6]^{3-/4-}$ using GCE, Graphene/GCE, GNPs/GCE and Graphene-GNPs/GCE.

Electrochemical impedance spectroscopy (EIS) was further used for the evaluation of modified electrode [36]. Figure 4 shows the Nyquist diagrams of different materials modified GCE in the presence of 0.01 M $[Fe(CN)_6]^{3-/4-}$. Due to the low electrocatalytic activity of GCE towards $[Fe(CN)_6]^{3-/4-}$, the bare GCE exhibits the largest semicircle domain present. After modification with Graphene-GNPs nanohybrids (as well as graphene or GNPs) on GCE, a decrease in electron transfer resistance

was observed, which may be caused by the fast electron transfer and excellent electrocatalytic of Graphene-GNPs nanohybrids. Compared to GNPs/GCE and Graphene/GCE, Graphene-GNPs/GCE display the smallest semicircle domain present, indicating the fastest electron transfer and/or best electrocatalytic of Graphene-GNPs nanohybrids. This phenomenon may be explained by the synergistic catalysis effect of graphene and GNPs on the surface of GCE. And this result is basically agreed with the DPV responses of different materials modified GCEs. Therefore, Graphene-GNPs nanohybrids were selected as the modification materials to construct electrochemical sensor for highly sensitive electrochemical detection of MG.

In order to investigate the possible electrode reaction mechanism, the study of scan rate (range from 10 to 500 mV/s) effect on peak current of 1 mM $K_3Fe(CN)_6$ in 0.10 M KCl electrolyte has been done by cyclic voltammetry method [37]. As shown in Figure 5a, a progressive increase in both anodic and cathodic peaks was observed with the increase of scan rates. As shown in Figure 5b, there is also a good linear relationship between the cathodic peak currents and square root of scan rate in the range of 10-500 mV/s. It can be given by the linear equation: y=1.24 x+7.6109 (R^2=0.9922). It reveals that the reaction of MG on Graphene-GNPs/GCE was controlled by the surface diffusion, in agreement with the quasi-reversible system. The active surface area of Graphene-GNPs/GCE was estimated according to the Randles-Sevcik equation [38]:

$$I_p = 2.69 * 10^5 * n^{3/2} * A * D^{1/2} C * \nu^{1/2}.$$

Where Ip is the peak current (A), n is the number of electrons transferred, ν is the scan rate (V/s), D the diffusion coefficient, A is the electrode area and C is the concentration of $K_3Fe(CN)_6$ solution. For 1 mM $K_3Fe(CN)_6$ in 0.1 M KCl electrolyte, n=1 and D=7.6*10^{-6} m/s. The active surface area of Graphene-GNPs/GCE was calculated to be 0.0547 cm^2.

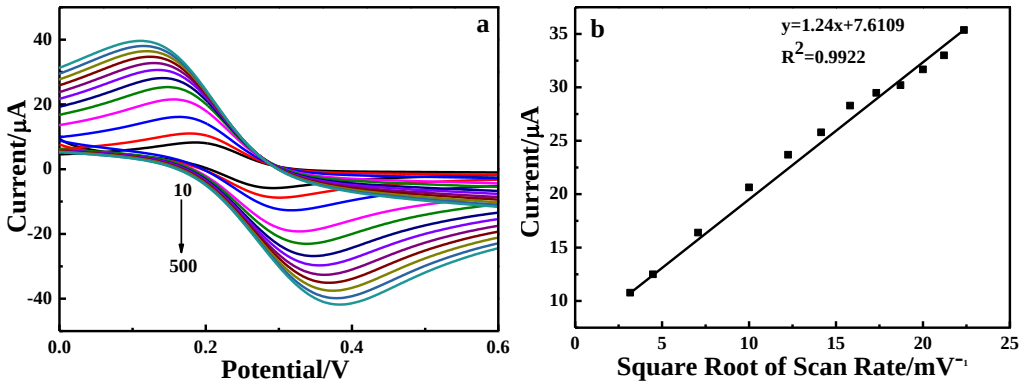

Figure 5. Cyclic voltammograms (a) and cathodic peak currents versus square root of scan rate plot (b) for Graphene-GNPs/GCE.

3.3. Optimization for determination condition

The oxidation peak current of MG is closely related to the pH value of the electrolyte solution. In this work, the oxidation peak current of MG (200 μM) at Graphene-GNPs/GCE were examined in Phosphate Buffered Saline (PBS) solutions with the pH values range from 5.5 to 8.5. Figure 5 shows the influence of pH values of PBS solutions on the electrochemical response of Graphene-GNPs/GCE

towards MG by DPV method. It was obviously that the DPV peak current of MG increased with increasing pH from 5.5 to 7.5 and then decreased with further increasing pH to 8.5. The highest DPV peak value of MG on Graphene-GNPs/GCE was obtained at pH=7.5. Therefore, PBS solution with a pH value of 7.5 was used as the supporting electrolyte for MG determination in the subsequent electrochemical experiments.

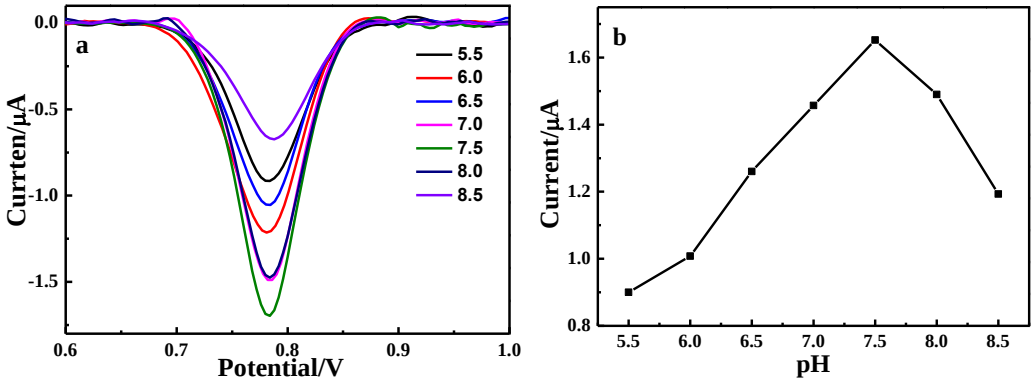

Figure 6. (a) DPV current of MG at Graphene-GNPs/GCE in PBS buffer with different pH values, (b) Relationship between DPV peak current and pH values of PBS buffer.

3.4. Electrochemical detection of MG

To investigate the application potential of the proposed Graphene-GNPs nanohybrids in electrochemical detection of MG, the DPV responses of MG solutions in the concentration range from 0.1 to 800 μM were investigated under optimized condition. As shown in Figure 7a, the DPV responses of MG on Graphene-GNPs/GCE increased as the concentration of MG increased in the whole range from 0.1 to 800 μM. The DPV peak current values were extracted from the DPV responses of Graphene-GNPs/GCE to different MG solutions and shown in Figure 6b. Obviously, the DPV peak current values of MG showed outstanding linear dynamic ranges from 0.1 μM to 800 μM with regression equation of y=0.0727 x+1.9523 (R^2=0.9916, n=3), where x is the concentration of MG and y is the DPV peak current value.

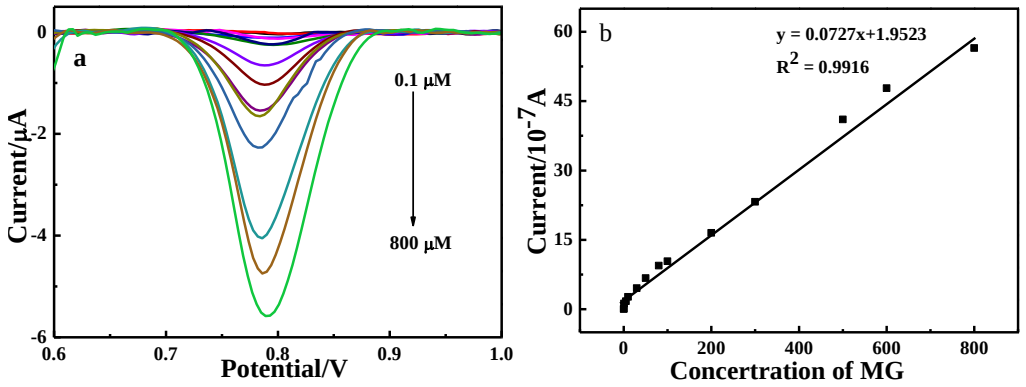

Figure 7. DPV responses of Graphene-GNPs/GCE based electrochemical sensor to MG solutions in the range from 0.1 μM to 800 μM (a). Calibration plots of DPV responses as a function of MG concentration (b).

In addition, a comparison of our proposed Graphene-GNPs/GCE based electrochemical sensor with other similar electrochemical sensors for MG also has been summarized and given in Table 1 [12,18-20,39-43]. From Table 1, we can find that our proposed method shows relatively higher sensitivity and/or wider linear range than other reported MG electrochemical sensors. Though some carbon paste electrodes based electrochemical sensors show relatively higher sensitivity than our proposed method[18, 42-43], their repeatability and/or stability issues can't be ignored, which may hinder their use in MG detection in the future. It should be noted that our proposed Graphene-GNPs/GCE based electrochemical sensor possess the widest linear range among all the electrochemical sensors for MG.

Table 1. Comparison of different electrochemical sensors for MG.

Modified electrode	Technique	Linear range (μM)	Reference
GCE	DPV	0.2-1.2	[12]
CPE	SWV	0.001-0.51	[18]
CPB/MWCNTs/GCE	CV	0.001-5	[19]
CeO_2/Nafion/GCE	SWASV	1-4	[20]
MWNTs /GCE	DPV	0.05-8	[39]
BDD film	CV	1-100	[40]
GQDs–Au/GCE	DPV	0.4-10	[41]
GO/En/CPE	DPV	0.008-0.8	[42]
SDBS/CPE	DPV	0.008-0.5	[43]
Graphene-GNPs/GCE	DPV	0.1-800	This work

3.5. Selectivity, repeatability and stability of Graphene-GNPs/GCE based electrochemical sensor

To confirm the selectivity of the proposed Graphene-GNPs/GCE based electrochemical sensor, an interference study was conducted by the determination of 100 μM MG in the presence of 100-fold of different foreign inorganic ions under the optimum conditions. Generally, a wide range of inorganic ions can be present in natural waters like river waters. The most frequently cations and anions found in river waters, Ca^{2+}, Mg^{2+}, Na^{+}, K^{+}, CO_3^{2-}, SO_4^{2-}, Cl^{-} and NO_3^{-} were chosen [44]. As shown in Figure 8, these foreign inorganic ions had no evidently influence on the detection of MG. Additionally, 50-fold concentration of ascorbic acid, uric acid, dopamine and caffeine also had no influence on the signals of MG with deviations below 10 %. These results demonstrate that the proposed electrochemical sensor had excellent selectivity for the determination of MG.

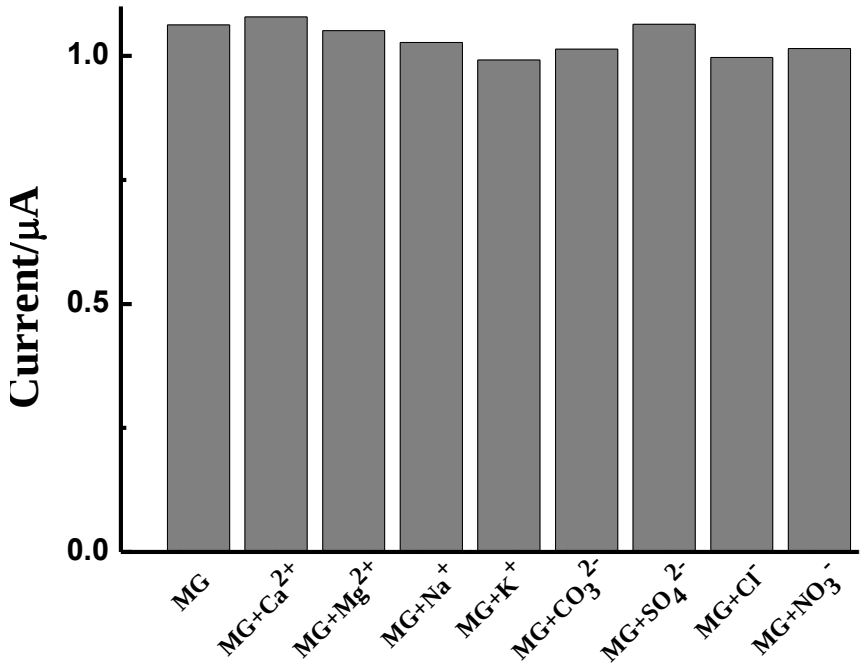

Figure 8. The selectivity of Graphene-GNPs/GCE based electrochemical sensor towards MG in the presence of some foreign inorganic ions

The repeatability of the proposed Graphene-GNPs/GCE based electrochemical sensor was evaluated by using the same electrode for 10 repeated analyzes of 100 μM MG. The DPV peak current values showed a relative standard deviation of 7.3 %, indicating the good repeatability of the Graphene-GNPs/GCE based electrochemical sensor. The stability of the Graphene-GNPs/GCE based electrochemical sensor was investigated by two different ways. When the Graphene-GNPs/GCE electrochemical sensor was exposed to surrounding atmosphere for 10 days at room temperature, the electrochemical sensor also reserved 87.6 % of its original response to 100 μM MG. The stability of the Graphene-GNPs/GCE electrochemical sensor is also evaluated within 2 weeks by recording the DPV peak current values once each day. The DPV peak current values of MG on Graphene-GNPs/GCE electrochemical sensor also retained 85.1 % of its initial current after 2 weeks. These results demonstrated that the prepared Graphene-GNPs/GCE electrochemical sensor had excellent repeatability and stability.

3.6. Determination of MG in real samples

In order to assess the suitability of the proposed Graphene-GNPs/GCE electrochemical sensor, the proposed methodology was tested through the determination of MG in real river waters by standard addition method. The obtained results were listed in Table 2. As it can be seen, the recoveries of MG in real river waters ranged from 97.5 % to 109.6 %, while relative standard deviation (RSD) ranged from 0.35 % to 5.57 %, suggesting an acceptable detection result for MG analysis in real river waters.

Table 2. Detection of MG in real river waters (n=3)

Added(μM)	Detected(μM)	Recovery (%)	R.S.D.(%)
1	1.03	102.8	2.32
5	5.48	109.6	5.57
10	9.95	99.5	0.45
30	29.25	97.5	0.35
50	49.17	98.3	4.18
100	100.12	100.1	1.45
400	404.23	101.0	1.40
600	611.01	101.8	0.72

4. CONCLUSIONS

In this work, we demonstrated a novel electrochemical sensor for detection of MG was fabricated based on Graphene-GNPs modified GCE. The Graphene-GNPs were prepared by simple chemical co-reduction of Au (III) and GO with sodium citrate. Owing to the excellent conductivity of graphene as well as superior electrocatalytic activity of GNPs, the proposed Graphene-GNPs/GCE electrochemical sensor displayed excellent stability, sensitivity, selectivity and repeatability towards MG. Furthermore, the proposed Graphene-GNPs/GCE based electrochemical sensor was applied for the determination of MG in real river waters. The satisfied results indicated that Graphene-GNPs will be promising electrode modification materials for determination of MG in other complex matrix as well as determination other pollutants in pharmaceutical or food.

ACKNOWLEDGEMENT
This study was funded by the Joint Talent Cultivation Funds of NSFC-HN (U1204214), the National Natural Science Foundation of China (21203053, 41206076), National key research and development program of China (2016YFC1400803 and 2016YFC1600801), the Innovation Research Team of Science and Technology in Henan province (16IRTSTHN019), the Young Key Teacher Foundation of Henan Province's Universities (2015GGJS-022), the Key Scientific Research Project of Henan Province's Universities (16A360017), the Science and Technology Development Project of Kaifeng (1503006) and the Scientific Research Foundation of Henan University (B2010079 and B2011037).

References

1. Khan A, UN appeals for aid for Sudan's humanitarian crisis. 2004.
2. D. J. Alderman, *J. Fish Dis*., 8 (1985) 289.
3. D. J. Alderman and R. S. Clifton-Hadley, *J. Fish Dis*., 16 (1993) 297.
4. R. A. Schnick, *The Progressive Fish-Culturist*, 50 (1988) 190.
5. B. Morteza, K. Foroogh and N. M. Peyman, *Talanta*, 85 (2011) 891.
6. A. R. Shalaby, W. H. Emam and M. M. Anwar, *Food Chem*., 226 (2017) 8.
7. Y. Jiang, P. Xie and G. Liang, *Aquaculture*, 288 (2009) 1.
8. S. Srivastava, R. Sinha and D. Roy, *Aquat. Toxicol*., 66 (2004) 319.
9. S. J. Culp, L. R. Blankenship, D. F. Kusewitt, D. R. Doerge, L. T. Mulligan and F. A. Beland,

Chem.-Biol. Interact., 122(1999) 153.
10. 2002/657/EC Commission Decision of 12 August 2002, Implementing Council Directive 96/23/EC, Brussels, *Off. J. Eur. Commun. L*., 221 (2002) 8.
11. S. Lee, J. Choi, L. X. Chen, B. Park, J. B. Kyong, G. H. Seong, J. Choo, Y. J. Lee, K. H. Shin, E. K. Lee and S. W. Joo, *Anal. Chim. Acta*., 590 (2007) 139.
12. D. Zhu, Q. Li, K. C. Honeychurch, M. Piano and G. Chen, *Anal. Lett*., 49 (2016) 1436.
13. K. Mitrowska, A. Posyniak and J. Zmudzki, *J. Chromatogr*. A, 1089 (2015) 187.
14. L. G. Noelia, R. G. Roberto, L. M. V. José and G. F. Antonia, *Ana. Methods*, 5 (2013) 3434.
15. F. Jia, X. Yang and Z. Li, *RSC Adv*., 6 (2016) 92723.
16. J. T. Yuan, L. F. Liao, X. L. Xiao, B. He and S. Q. Gao, *Food Chem*., 113 (2009) 1377.
17. J. M. Arts, M. J. Van Baak, C. J. Elloit, S. A. Hewitt, J. Cooper, K. Van d Velde-Fase and R. F. Witkamp, *Analyst*, 123 (1998) 2579.
18. K. M. Qu, X. Z. Zhang, Z. X. Lv, M. Li, Z. G. Cui, Y. Zhang, B. J. Chen, S. S. Ma and Q. Kong, *Int. J. Electrochem. Sci*., 7 (2012) 1827.
19. L. Q. Liu, F. Q. Zhao, F. Xiao and B. Z. Zeng, *Int. J. Electrochem. Sci*., 4 (2009) 525.
20. A. M. Sacara, C. Cristea and L. M. Muresan, *J. Electroanal. Chem*., 792 (2017) 23.
21. K. S. Novoselov, A. K. Geim, S. V. Morozov, D. Jiang, Y. Zhang, S. V. Dubonos, I. V. Grigorieva and A. A. Firsov, *Science*, 306 (2004) 666.
22. A. C. Ferrari1, J. C. Meyer, V. Scardaci, C. Casiraghi, M. Lazzeri, F. Mauri, S. Piscanec, D. Jiang, K. S. Novoselov, S. Roth and A. K. Geim. *Phys. Rev. Lett*., 97 (2006) 187401.
23. Y. B. Zhang, Y. W. Tan, H. L. Stormer and P. Kim, *Nature*, 438 (2005) 197.
24. P. Bollella, G. Fusco, C. Tortolini, G. Sanzò, G. Favero, L. Gorton and R. Antiochia, *Biosens. Bioelectron.*, 89 (2017) 152.
25. Y. M. Liang, L. L. Yu, R. Yang, X. Li, L. B. Qu and J. J. Li, *Sens. Actuators* B, 240 (2017) 1330.
26. X. C. Guo, H. H. Wang, X. J. Chen, Z. Y. Xia, W. Y. Kang and W. H. Zhou, *Int. J. Electrochem. Sci.*, 12 (2017) 861.
27. J. L. Bai, X. Y. Zhang, Y. Peng, X. D. Hong, Y. Y. Liu, S. Y. Jiang, B. A. Ning and Z. X. Gao, *Sens. Actuators* B, 238 (2017) 420.
28. H. W. Wang, S. Yao, Y. Q. Liu, S. L. Wei, J. W. Su and G. X. Hu, *Biosens. Bioelectron*., 87 (2017) 417.
29. N. Xia, X. Wang, J. Yu, Y. Y. Wu, S. C. Cheng, Y. Xing and L. Liu, *Sens. Actuators* B, 239 (2017) 834.
30. W. J. Lian, S. Liu, J. H. Yu, X. R. Xing, J. Li, M. Cui and J. D. Huang, *Biosens. Bioelectron*., 38 (2012) 163.
31. W. S. Hummers and R. E. Offeman, *J. Am. Chem. Soc*., 80 (1958) 1339.
32. G. Goncalves, P. A. A. P. Marques, C. M. Granadeiro, H. I. S. Nogueira, M. K. Singh and J. Grácio, *Chem. Mater*., 21 (2009) 4796.
33. S. J. Li, D. H. Deng, Q. Shi, *Microchim. Acta*, 177 (2012) 325.
34. Y. Tian, H. Q. Liu, G. H. Zhao and T. Tatsuma, *J. Phys. Chem*. B, 110 (2006) 23478.
35. Y. Wang, S. Zhang, D. Du, Y. Y. Shao, Z. H. Li, J. Wang, M. H. Engelhard, J. H. Li, Y. H. Lin, *J. Mater. Chem.*, 21 (2011) 5319.
36. X. F. Zhang, X. Z. Du, X. Huang and Z. P. Lv, *J. Am. Chem. Soc*., 135 (2013) 9248.
37. J. H. Li, Z. F. Xu, M. Q. Liu, P. H. Deng, S. P. Tang, J. B. Jiang, H. B. Feng, D. Qian and L. Z. He, *Biosens. Bioelectron*., 90 (2017) 210.
38. J. M. Gu, Y. H. Gao, J. X. Wu, Q. Li, A. X. Li, W. Zhang, H. Y. Dong, B. Wen, F. M. Gao and Y. S. Zhao, *ACS Appl. Mater. Interfaces*., 9 (2017) 8891.
39. H. C. Yi, W. Y. Qu, W. S. Huang, *Microchim. Acta*, 160 (2008) 291.
40. P. Ngamukot, T. Charoenraks, O. Chailapakul, S. Motomizu, S. Chuanuwatanakul, *Anal. Sci.*, 22 (2006) 111.
41. J. Y. Hou, F. Bei, M. L. Wang, S. Y. Ai, *J. Appl. Electrochem.*, 43 (2013) 689.

42. K. Zhang, G. Song, L. X. Yang, J. Zhou, B. X. Ye, *Anal. Methods*, 4 (2012) 4257.
43. W. S. Huang, C. H. Yang, W. Y. Qu, S. H. Zhang, *Russ. J. Electrochem*., 44 (2008) 946.
44. N. F. Robaina, L. G. T. dos Reis, R. J. Cassella, *Talanta*, 85 (2011) 749.